

# Strong effect of crystal structure on the proximity effect between a superconductor and monolayer of cobalt

Cite as: Appl. Phys. Lett. **121**, 231605 (2022); <https://doi.org/10.1063/5.0130313>

Submitted: 11 October 2022 • Accepted: 26 November 2022 • Published Online: 09 December 2022

Loïc Mougel, Patrick M. Buhl,  Qili Li, et al.



View Online



Export Citation



CrossMark

## ARTICLES YOU MAY BE INTERESTED IN

[One-dimensional bandgap modulation at continuous few-layer MoS<sub>2</sub> steps](#)

Applied Physics Letters **121**, 233103 (2022); <https://doi.org/10.1063/5.0117436>

[Fluoride ligand exchange for quantum dot light-emitting diodes with improved efficiency and stability](#)

Applied Physics Letters **121**, 231105 (2022); <https://doi.org/10.1063/5.0128318>

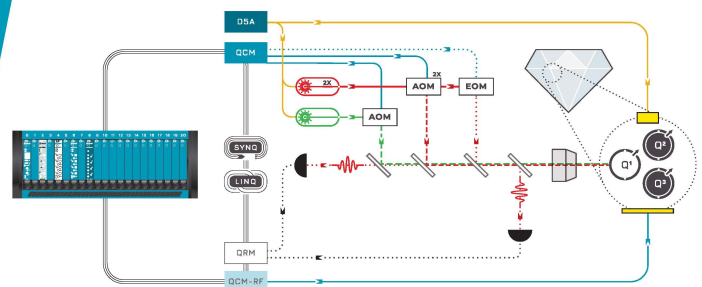
[Exciton-polaritons of hBN/WS<sub>2</sub> heterostructure in cavity observed at room temperature](#)

Applied Physics Letters **121**, 231106 (2022); <https://doi.org/10.1063/5.0118834>

 QBLOX

Integrates all  
Instrumentation + Software  
for Control and Readout of  
**NV-Centers**

[visit our website >](#)



# Strong effect of crystal structure on the proximity effect between a superconductor and monolayer of cobalt

Cite as: Appl. Phys. Lett. **121**, 231605 (2022); doi: [10.1063/5.0130313](https://doi.org/10.1063/5.0130313)

Submitted: 11 October 2022 · Accepted: 26 November 2022 ·

Published Online: 9 December 2022



View Online



Export Citation



CrossMark

Loic Mougel,<sup>1</sup> Patrick M. Buhl,<sup>2</sup> Qili Li,<sup>1</sup>  Anika Müller,<sup>1</sup> Hung-Hsiang Yang,<sup>1</sup>  Matthieu J. Verstraete,<sup>3</sup>   
Pascal Simon,<sup>4</sup>  Bertrand Dupé,<sup>5,6</sup> and Wulf Wulfhekel<sup>1,a)</sup> 

## AFFILIATIONS

<sup>1</sup>Physikalisches Institut, Karlsruhe Institute of Technology, 76131 Karlsruhe, Germany

<sup>2</sup>Institute of Physics, Johannes Gutenberg University Mainz, 55099 Mainz, Germany

<sup>3</sup>Nanomat/Q-mat/CESAM and European Theoretical Spectroscopy Facility, Université de Liège, B-4000 Sart Tilman, Belgium

<sup>4</sup>Laboratoire de Physique des Solides, UMR 8502, CNRS, Université Paris-Sud, Université Paris-Saclay, 91405 Orsay, France

<sup>5</sup>Fonds de la Recherche Scientifique (FNRS), B-1000 Bruxelles, Belgium

<sup>6</sup>Nanomat/Q-mat/CESAM, Université de Liège, B-4000 Sart Tilman, Belgium

<sup>a)</sup>Author to whom correspondence should be addressed: [wulf.wulfhekel@kit.edu](mailto:wulf.wulfhekel@kit.edu)

## ABSTRACT

We present an unexpectedly strong influence of the proximity effect between the bulk Ru(0001) superconductor and atomically thin layers of Co on the crystal structure of the latter. The Co monolayer grows in two different modifications, such as hcp stacking and a reconstructed  $\varepsilon$ -like phase. While hcp islands show a weak proximity effect on Co and a little suppression of superconductivity in the substrate next to it, the more complex  $\varepsilon$ -like stacking becomes almost fully superconducting. We explain the weak proximity effect between Ru and hcp Co and the rather abrupt jump of the superconducting order parameter by a low transparency of the interface. In contrast, the strong proximity effect without a jump of the order parameter in the  $\varepsilon$ -like phase indicates a highly transparent interface. This work highlights that the proximity effect between a superconductor and a normal metal strongly depends on the crystal structure of the interface, which allows to engineer the proximity effect in hybrid structures.

© 2022 Author(s). All article content, except where otherwise noted, is licensed under a Creative Commons Attribution (CC BY) license (<http://creativecommons.org/licenses/by/4.0/>). <https://doi.org/10.1063/5.0130313>

The superconducting proximity or Holm–Meissner effect is a phenomenon that arises when a normal metal is placed in contact with a superconductor<sup>1</sup> and can be used to engineer  $\pi$ -junctions in Josephson contacts for quantum devices.<sup>2–4</sup> While the normal metal can be described in the framework of Fermi liquid theory, in the superconductor, a gap appears in the single particle spectrum near the Fermi level and electrons condense in Cooper pairs.<sup>5</sup> In conventional superconductors, the pairing energy is a consequence of an attractive interaction between electrons mediated by virtual phonon exchange.<sup>6</sup> The Cooper pairs form a condensate, whose density reflects the superconducting order parameter. Lateral variations of the Cooper pair density inside the superconductor arise on the length scale of the superconducting coherence length  $\xi = \frac{\hbar v_f}{\pi \Delta}$ , with  $v_f$  being the Fermi velocity and  $\Delta$  being the superconducting gap.

When bringing a superconductor in contact with a normal metal, Cooper pairs may be scattered into the normal conductor and unpaired electrons may be scattered into the superconductor. In the normal metal, the attractive interaction between electrons is absent and Cooper pairs decay into single electrons after traveling a characteristic coherence length  $\xi_n = \sqrt{\frac{D}{2\pi T}} \neq 0$ , where  $D$  is the electron diffusion coefficient and  $T$  is the temperature. If the normal metal is magnetically ordered,<sup>7</sup> the exchange interaction of size  $E_{ex}$  effectively scatters electrons (and Cooper pairs), resulting in shorter coherence lengths of the order of  $\xi_f = \sqrt{\frac{\hbar D_f}{E_{ex}}}$ . For Co  $\xi_f$  is about 3 nm,<sup>2–4</sup> as deduced from Josephson junctions with intermediate Co layers. As a consequence, when approaching the interface, the superconducting order parameter continuously decays from its bulk value far inside the

superconductor, leaks into the normal metal, and finally vanishes far inside the normal metal. The superconducting properties are, thus, transferred over some distance into the normal metal, and the order parameter in the superconductor is lowered near the interface.<sup>7–9</sup> Based on this, we expect a strong proximity effect in single monolayers of Co on Ru.

In studies of the superconducting proximity, the nature of the interface between the two materials is often neglected. When extending our considerations to an interface with limited transmission of electrons and Cooper pairs, a discontinuous jump in the order parameter arises at the interface.<sup>10–12</sup> For example, a fully reflective interface (zero transparency) leads to complete decoupling of both materials, a suppression of the proximity effect, and an abrupt change of the Cooper pair density. A fully transparent interface (unity transmission) would result in a smooth variation of the order parameter across the interface. A limited transmission of electrons due to band mismatch between the two materials is the general case, where the interface has a transparency below 1. In this case, on top of gradual changes inside both materials, an abrupt jump of the order parameter arises at the interface.<sup>10–12</sup>

In this work, we consider a crystalline superconductor–normal (SN) interface and show that the proximity effect can be changed drastically, depending on the interface to the normal metal. Our model system is Co on Ru(0001),<sup>13–15</sup> in which Co can grow either in the hcp phase, in registry with the crystal structure of Ru or in a  $\epsilon$ -like phase with a broad reconstruction which breaks the local translational invariance of the interface.

Co/Ru(0001) samples were prepared under ultra-high vacuum (UHV) at a base pressure of  $4 \times 10^{-11}$  mbar. The Ru(0001) single crystal was cleaned by cycles of annealing in oxygen and argon-ion sputtering followed by thermal annealing.<sup>14</sup> On the atomically flat and clean surfaces, Co films were deposited from an e-beam evaporator followed by a transfer to a scanning tunneling microscope (STM) under UHV. STM measurements were performed at 30 mK with a home-built microscope.<sup>16</sup>

In our previous work, we reported on the magnetic ground state of hcp Co on Ru(0001), which is a Bloch-type spin spiral.<sup>14</sup> Here, we show that, depending on the deposition parameters, two differently stacked phases appear. In addition to the hcp stacking of the Co layer, which forms triangular islands [see Fig. 1(a)], islands with opposite step edge orientation (reversed triangles) can be found [see Fig. 1(b)]. These islands appear about 50 pm lower in the STM images. Figure 1(c) shows a zoomed area with atomic resolution containing both phases. It was recorded near a Ru upward step edge (green arrows) with a narrow strip of hcp stacked Co surrounding it, which appears slightly darker. The crystal lattice going from Co to Ru shows no lateral shifts, confirming an identical hcp stacking (yellow lines). Next to the hcp Co, the second phase is visible that shows a different crystal structure. It is separated by a phase boundary (light blue arrows). The phase shows a large unit cell in the form of a  $(\sqrt{10} \times \sqrt{10})$ -reconstruction. The basis vectors are indicated by red arrows and have a length of 939 pm. This unit cell agrees well with the 2d unit cell of the rather open (111) surface of bulk  $\epsilon$ -Co of 860 pm (Ref. 17) as shown in an atomic model (gray spheres represent Co atoms) in Fig. 1(d). The positions of the atoms exposed to the vacuum in that unit cell are marked by green dots and agree qualitatively with the STM image [see the replica of position in Fig. 1(c)]. Note that the binary phase diagram

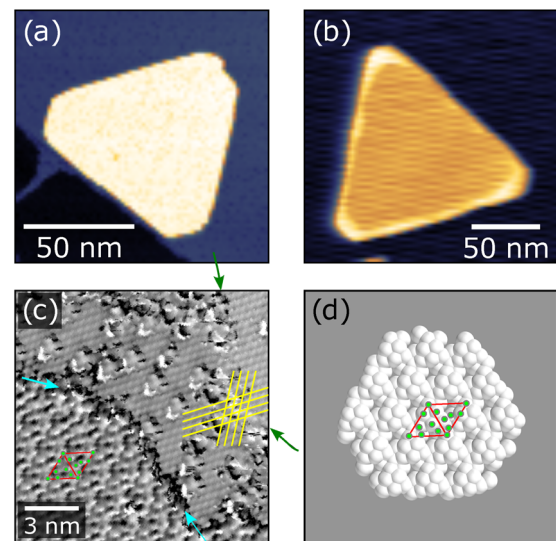


**FIG. 1.** Topographic images of two triangular Co islands of one atom thickness with different stackings on the Ru(0001) surface: (a) hcp and (b)  $\epsilon$  ( $U = 1$  V,  $I = 1$  nA). (c)  $dI/dz$  image of the different stackings of Co near a Ru(0001) step edge ( $U = 100$  mV,  $I = 1$  nA, and  $z_{mod} = 20$  pm). The green and light blue arrows denote step edges and domain boundaries of the stacking, respectively (see the text) and the yellow lines highlight rows of Co and Ru atoms visible on the hcp Ru and Co surface. (d) (111) cut of  $\epsilon$ -Co phase. The red diamond shows the unit cell. The green dots show the positions of the surface Co atoms. The positions are repeated in (c) for comparison.

of Co and Ru contains a phase designated as  $\epsilon$ ,<sup>18</sup> but it differs from the phase we observe here. The  $\epsilon$ -phase we observe was also found for pure Co in small clusters and was shown to order ferromagnetically similar to hcp Co.<sup>17,19</sup> The Co atoms in the unit cell are less densely packed than in the hcp lattice. Furthermore, the  $\epsilon$ -islands display a brighter, i.e., higher, border, as can be seen in Fig. 1(b). Atomically resolved images (not shown) identify this rim as hcp stacked Co.

Ru has a superconducting critical temperature of  $T_c = 470$  mK,<sup>20</sup> i.e., it is superconducting at the measurement temperature of 30 mK. To investigate the proximity effect between Ru and the Co islands, we recorded local tunneling spectra. Figures 2(a) and 2(d) show individual  $dI/dU$  spectra recorded in three positions as indicated by the color code. The insets of Figs. 2(b) and 2(e) show the individual hcp and  $\epsilon$ -islands as well as the line sections on which the spectra were taken.

Next to both islands and on the Ru substrate, the spectra (blue lines) show a superconducting gap of  $\Delta = 60.7 \pm 0.7$   $\mu$ eV, which is slightly lower than our previous measurements on bare Ru(0001).<sup>16</sup> As expected, superconductivity of the bulk Ru sample is not quenched by the monolayer islands of Co. Additionally, the gap is incomplete, i.e., the differential conductance does not vanish at zero bias. This can be easily explained by the estimated coherence length for Ru is  $\xi = \frac{\hbar v_f}{\pi \Delta} = 3.4$   $\mu$ m. This is much larger than the average Co island size and their separation. Thus, the effect of the islands on superconductivity of the bulk substrate is spatially averaged and the gap on the free Ru surface is consistently reduced by a small amount on the whole surface due to the proximity effect.

Placing the tip on the island edge, the behavior of hcp and  $\epsilon$ -islands is similar (green lines). The zero-bias conductance is

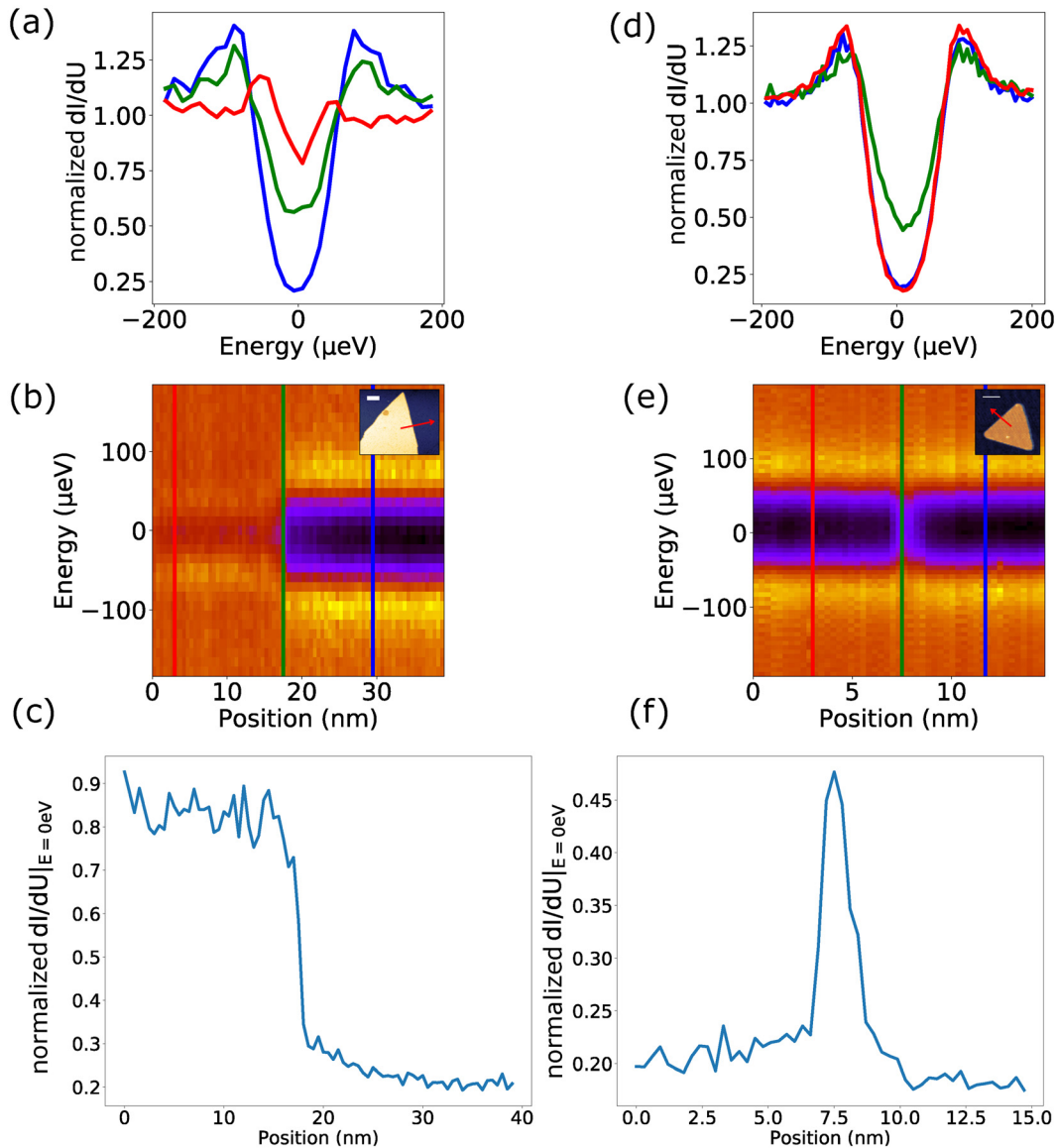


**FIG. 2.**  $dI/dU$  scans of the Co monolayers on Ru. Left panels: hcp-Co. Right panels:  $\epsilon$ -Co. (a) and (d) Individual  $dI/dU$  spectra recorded on free Ru (blue), edge of the island (green), and on the bulk of the island (red). The line profiles are extracted from the  $dI/dU$  spectra visible on (b) and (e). (b) and (e) Color coded  $dI/dU$  spectra plotted against lateral position of the tip crossing the island edge. The left halves of the spectra are recorded on the island, while the right halves are recorded on free Ru. The insets show the topographic images of the islands on which the spectra were recorded. The red line shows the scan trajectory of the tip. (c) and (f) The  $dI/dU$  value at the Fermi energy plotted against the position of the tip. All  $dI/dU$ -data were normalized to the differential conductance at an energy of 300  $\mu\text{eV}$ .

drastically increased, i.e., the Cooper pair density is significantly decreased, although the spectra were recorded on only a single atom thick Co layer. Measuring inside the islands (red lines), however, the spectra differ dramatically. While on the  $\epsilon$ -island the spectrum is almost identical to that of the bare Ru, on the hcp island, we find a reduction in the gap intensity, much stronger than expected from the coherence length  $\xi_f \approx 3$  nm reported in the literature for Co.<sup>2-4</sup> Furthermore, inside the gap states evolve that are slightly asymmetric with a peak structure above and below the Fermi energy. Such a

behavior is often attributed to Yu–Rusinov–Shiba (YRS) states,<sup>21-24</sup> when a magnetic metal or impurity is brought into contact with a superconductor. Note that due to the islands size of many thousands of Co atoms, no single YRS states but a continuum is expected that also may depend on the magnetic configuration inside the island such that systematic study of this goes beyond the scope of this paper.

Figures 2(b) and 2(e) show color coded  $dI/dU$  spectra as a function of lateral displacement when going from the island (left) over the edge to the bare substrate (right). First, we note that the reduced gap

on the edge of the  $\varepsilon$ -island coincides with the bright rim observed in the STM topography and coincide with the hcp rim of the island. This explains the similar spectra for the two island edges.

Figures 2(b) and 2(e) give a more detailed view of the tunneling spectra as a function of position. In both contour plots, the spectra evolve continuously when going from the substrate over the edge and into the island. Notably, the positions of the coherence peaks shift to slightly lower energies when coming close to the islands. At the same time, the  $dI/dU$  signal at zero bias increases gradually over a distance of a few nm. To analyze this, we plot  $dI/dU$  at zero bias as a function of position [see Figs. 2(c) and 2(f)].

For the magnetic hcp island, the quasi-particle density starts a gradual increase about  $\approx 15$  nm before the island edge, then abruptly jumps at the edge and is essentially constant on the island. The first effect can be simply explained by the dimensionality  $n$  of the problem. In general, the proximity effect leads to variations of the Cooper pair density in a superconductor with the function  $|\psi|^2 \approx r^{-(n-1)} e^{-r/\xi}$ , i.e., for a one-dimensional problem, the usual exponential decay is found, while for higher dimensions, the scattering geometry has to be considered. For a three-dimensional situation, the  $1/r^2$  factor simply represents particle conservation. We do not attempt to fit the dependence: first of all,  $\xi$  is so large that no meaningful number can be fit on sections of a length of only a few nm; and second, the dimensionality of the problem near an island should display a crossover from two to three-dimensional. Essentially, the same behavior is found for the hcp rim of the  $\varepsilon$ -island.

The second effect, i.e., the sudden jump, however, calls for another explanation. As discussed in the introduction, for a fully transparent interface, the order parameter varies smoothly, which is at odds with the observation. Instead, it jumps abruptly when going from the substrate to the Co monolayer. Assuming that the order parameter in Ru below the island varies smoothly on the characteristic length scale implies that it needs to jump to the much reduced value observed on the Co monolayer at the Ru/Co interface indicating a partial transmission of electrons at the interface. The interface, thus, largely decouples the two regions. Note that a fully transparent interface would either lead to a strong reduction of the superconducting order parameter in Ru (below and near the island) or a stronger proximity effect in the Co island, as observed in  $\pi$ -junctions of Nb and Co.<sup>3,4</sup>

In contrast, the  $\varepsilon$ -island shows only slightly higher differential conductance at zero bias than the bare substrate. This indicates a strong proximity effect and nearly the same order parameter as the substrate. The interface must be highly transparent.

In conclusion, we have shown that Co grows in two different stackings on a Ru(0001) substrate. Co in the pseudomorphic hcp stacking shows strongly suppressed superconductivity while the  $\varepsilon$ -phase exhibits a similar Cooper pair density as the substrate. This behavior is explained by a reflective interface for hcp Co limiting the proximity effect while the  $\varepsilon$ -phase with its almost full gap hints for a large transparency. The influence of the crystal interface can be used to engineer proximity effect in hybrid structures<sup>12</sup> to tune hybridization of the states, for example, in superconducting spin valves and  $\pi$ -junctions.<sup>7</sup> The transparency effect is expected to be of paramount importance especially for crystalline interfaces.

W. Wulfhekel acknowledges funding by the Deutsche Forschungsgemeinschaft (DFG) under Grant Nos. WU 349/15-1

and WU 349/16-1. H. S. Yang acknowledges funding by the Alexander-von-Humboldt Foundation. B. Dupé and P. Buhl acknowledge funding by the DFG under Grant No. DU 1489/3-1.

## AUTHOR DECLARATIONS

### Conflict of Interest

The authors have no conflicts to disclose.

### Author Contributions

**Loic Mougél:** Conceptualization (equal); Investigation (equal); Visualization (equal); Writing – original draft (equal). **Patrick Buhl:** Conceptualization (equal); Writing – review & editing (equal). **Qili Li:** Investigation (equal). **Anika Müller:** Data curation (equal); Investigation (equal). **Hung-Hsiang Yang:** Formal analysis (equal); Investigation (equal). **Matthieu Verstraete:** Conceptualization (equal); Writing – review & editing (equal). **Pascal Simon:** Conceptualization (equal); Writing – review & editing (equal). **Bertrand Dupé:** Conceptualization (equal); Writing – review & editing (equal). **Wulf Wulfhekel:** Conceptualization (equal); Funding acquisition (equal); Investigation (equal); Resources (equal); Writing – original draft (equal).

## DATA AVAILABILITY

The data that support the findings of this study are available from the corresponding author upon reasonable request.

## REFERENCES

- <sup>1</sup>R. Holm and W. Meissner, “Messungen mit Hilfe von flüssigem helium. XIII,” *Z. Phys.* **74**, 715–735 (1932).
- <sup>2</sup>J. W. A. Robinson, S. Piano, G. Burnell, C. Bell, and M. G. Blamire, “Critical current oscillations in strong ferromagnetic  $\pi$  junctions,” *Phys. Rev. Lett.* **97**, 177003 (2006).
- <sup>3</sup>M. A. Khasawneh, W. P. Pratt, and N. O. Birge, “Josephson junctions with a synthetic antiferromagnetic interlayer,” *Phys. Rev. B* **80**, 020506 (2009).
- <sup>4</sup>T. S. Khaire, M. A. Khasawneh, W. P. Pratt, and N. O. Birge, “Observation of spin-triplet superconductivity in Co-based Josephson junctions,” *Phys. Rev. Lett.* **104**, 137002 (2010).
- <sup>5</sup>L. N. Cooper, “Bound electron pairs in a degenerate Fermi gas,” *Phys. Rev.* **104**, 1189–1190 (1956).
- <sup>6</sup>J. Bardeen, L. N. Cooper, and J. R. Schrieffer, “Microscopic theory of superconductivity,” *Phys. Rev.* **106**, 162–164 (1957).
- <sup>7</sup>A. I. Buzdin, “Proximity effects in superconductor-ferromagnet heterostructures,” *Rev. Mod. Phys.* **77**, 935–976 (2005).
- <sup>8</sup>P. De Gennes and E. Guyon, “Superconductivity in ‘normal’ metals,” *Phys. Lett.* **3**, 168–169 (1963).
- <sup>9</sup>N. R. Werthamer, “Theory of the superconducting transition temperature and energy gap function of superposed metal films,” *Phys. Rev.* **132**, 2440–2445 (1963).
- <sup>10</sup>G. E. Blonder, M. Tinkham, and T. M. Klapwijk, “Transition from metallic to tunneling regimes in superconducting microconstrictions: Excess current, charge imbalance, and supercurrent conversion,” *Phys. Rev. B* **25**, 4515–4532 (1982).
- <sup>11</sup>A. V. Bubis, A. O. Denisov, S. U. Piatrusha, I. E. Batov, V. S. Khrapai, J. Becker, J. Treu, D. Ruhstorfer, and G. Koblmüller, “Proximity effect and interface transparency in Al/InAs-nanowire/Al diffusive junctions,” *Semicond. Sci. Technol.* **32**, 094007 (2017).
- <sup>12</sup>C. Cirillo, S. L. Prischepa, M. Salvato, C. Attanasio, M. Hesselberth, and J. Aarts, “Superconducting proximity effect and interface transparency in Nb/PdNi bilayers,” *Phys. Rev. B* **72**, 144511 (2005).

- <sup>13</sup>F. E. Gabaly, J. M. Puerta, C. Klein, A. Saa, A. K. Schmid, K. F. McCarty, J. I. Cerda, and J. de la Figuera, "Structure and morphology of ultrathin Co/Ru(0001) films," *New J. Phys.* **9**, 80 (2007).
- <sup>14</sup>M. Hervé, B. Dupé, R. Lopes, M. Böttcher, M. D. Martins, T. Balashov, L. Gerhard, J. Sinova, and W. Wulfhekel, "Stabilizing spin spirals and isolated skyrmions at low magnetic field exploiting vanishing magnetic anisotropy," *Nat. Commun.* **9**, 1015 (2018).
- <sup>15</sup>L. Mougél, P. M. Buhl, R. Nemoto, T. Balashov, M. Hervé, J. Skolaut, T. K. Yamada, B. Dupé, and W. Wulfhekel, "Instability of skyrmions in magnetic fields," *Appl. Phys. Lett.* **116**, 262406 (2020).
- <sup>16</sup>T. Balashov, M. Meyer, and W. Wulfhekel, "A compact ultrahigh vacuum scanning tunneling microscope with dilution refrigeration," *Rev. Sci. Instrum.* **89**, 113707 (2018).
- <sup>17</sup>V. A. de la Peña O'Shea, I. d. P. R. Moreira, A. Roldán, and F. Illas, "Electronic and magnetic structure of bulk cobalt: The  $\alpha$ ,  $\beta$  and  $\epsilon$ -phases from density functional theory calculations," *J. Chem. Phys.* **133**, 024701 (2010).
- <sup>18</sup>W. Köster and E. Horn, "Zustandsbild und gitterkonstanten der legierungen des kobalts mit rhenium, ruthenium, osmium, rhodium und iridium," *Z. Metallk.* **43**, 444 (1952).
- <sup>19</sup>S. Sun and C. B. Murray, "Synthesis of monodisperse cobalt nanocrystals and their assembly into magnetic superlattices," *J. Appl. Phys.* **85**, 4325 (1999).
- <sup>20</sup>D. K. Finnemore and D. E. Mapother, "Absence of an isotope effect in superconducting ruthenium," *Phys. Rev. Lett.* **9**, 288–290 (1962).
- <sup>21</sup>L. Yu, "Bound state in superconductors with paramagnetic impurities," *Acta Phys. Sin.* **21**, 75–91 (1965).
- <sup>22</sup>H. Shiba, "Classical spins in superconductors," *Prog. Theor. Phys.* **40**, 435–451 (1968).
- <sup>23</sup>A. Rusinov, "Theory of gapless superconductivity in alloys containing paramagnetic impurities," *Sov. Phys. JETP* **29**, 1101–1106 (1969); available at [http://jetp.ras.ru/cgi-bin/dn/e\\_029\\_06\\_1101.pdf](http://jetp.ras.ru/cgi-bin/dn/e_029_06_1101.pdf)
- <sup>24</sup>A. V. Balatsky, I. Vekhter, and J.-X. Zhu, "Impurity-induced states in conventional and unconventional superconductors," *Rev. Mod. Phys.* **78**, 373 (2006).